Journal of Cleaner Production 437 (2024) 140761

Contents lists available at ScienceDirect

Journal of Cleaner Production

journal homepage: www.elsevier.com/locate/jclepro

Investigating the room- and cryo-milling impact in lignocellulosic biomass and its consequence over pyrolysis and oxidative treatments

Concepción Real Pérez [b], María Dolores Alcalá González [a], Francisca Romero Sarria [a], María del Carmen Hidalgo López [b], José Manuel Córdoba Gallego [a,*]

[a] Dpto. Química Inorgánica, Facultad de Química, Universidad de Sevilla (US), C/Prof. García González 1, 41012, Sevilla, Spain
[b] Instituto de Ciencia de Materiales de Sevilla (Universidad de Sevilla, Consejo Superior de Investigaciones Científicas), C/Américo Vespucio 49, 41092, Sevilla, Spain

ARTICLE INFO

Handling Editor: Panos Seferlis

Keywords:
Milling
Biomass
Recalcitrance
Liquid nitrogen
Green chemistry
IR spectra

ABSTRACT

The lignocellulosic biomass recalcitrance is the uppermost factor for the utilization of this renewable resource. The development of new pre-treatments, addressed to enhance performance in lignocellulosic biomass conversion into biofuels, fine chemicals, and as potential sources of building blocks for materials, must be focus in two main areas: effectiveness (cost-effective and chemical effective) and green chemistry. In this research, a set of different biomass sources (farmer, harvested wild trees and secondary products) were studied to evaluate the high efficiency of the non-liquid nitrogen (LN) and LN-treated biomass samples' planetary ball milling performance. The samples have been characterized by particle size distribution, thermogravimetric, FT-IR, statistical chemometric and chemical oxidation analysis. The results have shown a high level on the rupture of the crystallinity and depolymerization degrees of the cellulose and the lignin, for both, non-LN and LN-treated samples. The thermogravimetric analysis showed a clear diminishing in temperature degradation, and a larger amount of biomass degraded at lower temperature, as well as, a high chemical oxidation degree than not milled samples. Finally, the LN-treated samples even exhibited a lower degradation temperature, a larger amount of biomass degraded at lower temperature and a higher oxidation degree, than those non-LN milled.

1. Introduction

One of the greatest outfacing of our civilization is to overcome the higher scientific and economic hurdles to meet the growing demand for industrial chemical precursors and fuel. Since the previous century, a great effort has been done to find sources of chemicals and alternative energies alternatives to fossil fuels. Lignocellulosic substrates, which are carbon dioxide neutral and there is a great abundance of surplus material worldwide, are one of these new sources.

The world-wide production of accessible lignocellulosic biomass reaches about 10^{11} tons/year (Saini et al., 2015). The lignocellulosic material, based on the resources, could be classified into three main groups, such as municipal solid wastes, forest residues and crop residues (Taherzadeh and Karimi, 2008). The composition of lignocellulosic biomass varies from biomass source studied depending on the growth conditions, the plant species and the types of plant tissue, and it usually contains about 10–25% lignin, 35–50% cellulose and 20–35% hemicellulose (Sawant et al., 2016).

The lignin molecular configuration itself which makes it extremely resistant and un-reactive to hydrolysis (chemical and enzymatic) (Mussatto and Teixeira, 2010), joined to the crystallinity, the high polymerization degree of the cellulose and the degree of hemicellulose acetylation are the major obstacles in the effective utilization of the lignocellulosic biomass (Zoghlami and Paës, 2019). Therefore, all these potential sugar fractions are not straightly accessible for diverse treatments (e.g.: enzymatic treatment), and, for example, the biofuel or furfural production.

Several pretreatment methods have brought important effects to break down the crystalline structure in cellulose and the lignin structure, such as physicomechanical comminution (Arce and Kratky, 2022), ultrasound (Subhedar et al., 2016), high-energy radiation (Kristiani et al., 2015), high-pressure steam (Ziegler-Devin et al., 2021), hydrolysis (acid or alkaline) (Dubey et al., 2012), chemical (H_2O_2) (Gould, 1984), gas treatment (HClO, NO_2, SO_2, O_3) (Mulakhudair et al., 2017), wet oxidation (McGinnis et al., 1983), organo-solvent treatment (Nair et al., 2023), ammonia fiber expansion (Bals et al., 2010), ionic liquids (An

* Corresponding author.
E-mail address: jmcord@us.es (J.M. Córdoba Gallego).

https://doi.org/10.1016/j.jclepro.2024.140761
Received 20 November 2023; Received in revised form 10 January 2024; Accepted 12 January 2024
Available online 16 January 2024

et al., 2015), and biological treatment (Fan et al., 2010). Among all of them, chemical pretreatments are widely used, however, the high level of equipment investment, treatment cost and environmental pollution due to the use of a high amount of solvents (water or others) (Brodeur et al., 2011) results in the searching for a new green alternative.

The mechanical pretreatments, without the production of wastes, have appeared as an efficient way to improve, during the hydrolysis, the total digestibility and the depolymerization of saccharides. For example, studies have shown a higher level of digestibility, by a diminishing in the heat and mass transfer limitations, when the particle size of the biomass was reduced to 0.5–2 mm. Unfortunately, nowadays, the balance between the cost-effectiveness of the mechanical size reduction steps and the adding-value compounds production is unacceptable due to high-energy requirements of the process (Barakat et al., 2013).

The finest powders production is cost-intensive, or even not possible at room temperatures due to the viscoelastic and plastic properties of the biomass. At ambient temperature, the biomass fibre layer structure, with the presence of intermediate layers, exhibits high plasticity and extensibility and makes it high resistant to rupture by the effect of the impact forces applied during the grinding process. The grinding efficiency can be improved by lowering the working milling temperature as much as possible. The liquid nitrogen has the potential to become the best cooling agent (act very fast, a non-waste solution is produced and it is an inert agent) to reach the lowest working temperature for the milling procedure.

At first, under the cryogenic temperature condition many materials, such as biomass, become brittle and they can be grounded more effectively. Also, under these conditions enzyme activities in fresh plants are inactivated. Secondly, another mechanism to overcome the biomass recalcitrance and to improve the saccharification process, induced by the cryogenic grinding, is the rupture of the biomass microfibrils by the action of ice crystals pressure against the cell's walls induced by the impact forces applied during the milling procedure. The utilization of cryogenic grinding has numerous advantages in process application, such as, readily available, easy control, low technical input, good heat transition, inert atmosphere, better cost-effective to obtain finer particles, etc. and other advantages (Manohar and Sridhar, 2003; Hemery et al., 2011), from a physico-chemical characteristics point of view of the products obtained, such as, the activity of some specific compounds is preserved by the limitation of the heat generated during grinding (Hemery et al., 2011; Singh et al., 1999; Saxena et al., 2018; Goswami and Singh, 2003), and a lower particle size leads to a higher particle surface area and therefore to a higher interaction solvent-compounds interactions which can result in higher production of bioactive compounds (Stewart et al., 2009).

There is a race for scientific knowledge advancement and the technological optimization (cost, chemical, and green effectiveness) of the pre-treatment process, among them the grinding process, to produce biofuel and building blocks more efficiently from lignocellulosic resources. The main aim of the work is to show the effects of short time high efficiency planetary ball milling procedure in biomass assessed by particle size distribution, thermogravimetry, FTIR spectroscopy, statistical chemometric and chemical oxidation analysis to investigate the chemical structure changes produced by a given biomass material influenced by room temperature milling and cryo-milling. This study is expected to give useful information about the impact of room and cryo-temperature milling pretreatment on the biomass structure, considering the potential in the processes improvement.

2. Experimental

A set of different biomass sources (farmer, harvested wild tree and secondary products) were used in this work. They are shown in Table I. The morphology format of the as-received biomass was a set of particles with a size in the range from 3 to 5 mm. 30 g of every biomass source was added in a 250 ml (volume) plastic bottle with 50 ml of liquid nitrogen (LN). After the LN evaporation, the biomass was immediately poured in a stainless-steel jar (volume, 125 ml) with 9 stainless steel balls (diameter, 20 mm). The jar was closed and placed in a PM200 (Retsch, Germany) planetary ball milling. The PM200 speed was set as 500 rpm, and the milling time was fixed to 300 s. For comparison, as-received biomass was milled under similar conditions without previous LN treatment. The LN treated samples were called "T_{Cryo}" and the non-LN treated samples were called "T_{Room}".

Powdered biomass, obtained after milling at room temperature, was characterized by moisture content analysis and elemental analysis. The moisture content was performed by the oven-drying method in a Binder VD23 oven. The temperature was set at 105 °C for 48 h. The CHNS elemental analyses were carried out in a Micro Elemental Analyzer, using a LECO Truspec CHNS Micro. The samples were completely combusted in pure oxygen up to 1050 °C. The product gases obtained, CO_2, H_2O and SO_2 were quantified by an infrared cell, and by a thermal conductivity cell for the N_2. Three runs were carried out per sample.

The oxygen value was indirectly calculated by difference using the equation below (1) (Zhang et al., 2010):

$$\%O = 100 - \%H - \%C - \%N - S - \%ash \quad (1)$$

There are several mathematical equations, available in the literature, to determine the biomass High Heating Value (HHV). The estimated value can be reached from three types of experimental analysis: ultimate analysis data, proximate analysis data and structural analysis data (Vargas-Moreno et al., 2012). In this research, the Grabosky and Bain equation (2) (Broer et al., 2019) based on ultimate analysis data will be used. This equation, useful for a wide range of biomass materials, is based on the reaction to produced CO_2, H_2O, NO_2 and SO_2 from C, H, N and S, and its prediction is asserted to be within 1,5%. The C, H, N and S w.t.% used in this equation were those obtained from a biomass sample with moisture and ash.

Table 1
Moisture content, ash content, ultimate elemental analysis (w.t.% in dry basis and without ash), C/H ratio and HHV (high heating value) of samples studied in this work. The relative standard deviation (%) for the determined C; H; N; and S values was in the range of 0,4–1,4; 0,8–1,9; 2,7–5,5; and 3,9–6,5, respectively.

Sample	Code	%C	%H	%N	%S	%O	%ash	%moisture	C/H	HHV (kJ/g)
Cellulose	Cel	45,5	11,1	<0,1	<0,1	43,4	0	5,1	4,1	19,8
Lignin	Lig	53,8	8,6	<0,1	0,7	36,9	0	10,9	6,3	20,7
Cel:Lig 1:1	CL11	49,4	9,9	<0,1	<0,1	40,8	0	8,0	5,0	20,2
Cel:Lig 1:2	CL12	50,6	9,4	<0,1	0,6	39,5	0	8,9	5,4	20,3
Rice husk	RicHusk	41,2	5,3	<0,1	<0,1	53,5	17,1	7,2	7,8	12,1
Rice straw	RicStr	48,4	10,2	0,5	<0,1	40,9	18,8	8,4	4,7	15,7
Olive tree pruning	OliPru	49,6	7,2	0,7	<0,1	42,4	3,2	8,1	6,9	18,3
Wild olive tree pruning	WOliPru	50,6	6,0	0,7	0,7	41,9	3,0	10,6	8,4	17,6
Pine tree pruning	PinePru	52,5	6,4	0,4	<0,1	40,8	2,6	12,6	8,2	17,9
Eucalyptus tree pruning	EucPru	49,0	6,1	0,2	≤0,1	44,7	4,2	11,4	8,1	16,5
Peanut shell	PeaShe	40,6	5,0	<0,1	0,2	54,2	3,9	4,9	8,1	14,3
Wallnut shell	WalShe	50,7	6,3	<0,1	<0,1	43,0	2,6	8,6	8,1	18,2

$$HHV = 0,328\ C + 1,4306H - 0,0237N + 0.0929S - \left(1 - \frac{Ash}{100}\right) \bullet \left(\frac{40,11H}{C}\right) + 0,3466\ [\mathrm{J/g}] \quad (2)$$

Particle size distribution (PSD) was measured using a Mastersizer 3000E (Malvern, UK) laser diffraction granulometer. Particle size measurements were carried out by a wet-method with distilled water. The data was acquired using Mastersizer 3000E extended software. The GRADISTAT software (Blott and Pye, 2001) was used to compute different PSD numerical values. These values were classified in three groups: size parameters (geometric mean diameter ($\overline{x_D}$), D_{90}, median diameter (D_{50}) and effective diameter (D_{10})), shape parameters (skewness and kurtosis) and distribution parameters (geometric standard deviation (G_{SD})).

FT-IR studies were performed by a ThermoFisher FT-IR Nicolet™ iS™ 5 with resolution set on 1 cm^{-1} spectrometer was applied (range of 400–4000 cm^{-1}, and 64 co-added scans to reduce the random noise interference). The spectral data were acquired at room temperature and processed by the Omnic Thermo Scientific software (Thermo Fisher Scientific Inc., Waltham, MA, USA). Solid-state pellets (uniaxial press, 13 mm in diameter, 2 tons, 2 min, connected to a vacuum pump) made of KBr (FT-IR grade, ≥99% trace metals basis, Merck, Darmstadt, Germany) were used as a matrix thoroughly mixed with the studied powdered biomass sample in a handle-mortar. The ratio was approximately 1:10 mg (sample:KBr). The sample mass was registered for every pellet, and it was used to correct the FT-IR spectra intensity. 10 spectra were registered and averaged for every biomass sample studied. Because KBr powder is hygroscopic, it is dried at 105 °C and stored in special hermetic containers. The prepared pellets with the assessed material are dried for further 24 h. The pellets should be clear and evenly colored. Weak bands related to water can also be corrected by measuring the background spectrum using a KBr pellet of the same thickness but not comprising the examined item.

The following indexes were obtained from de FT-IR spectra bands: the LOI (B1422/B896, Lateral Order Index), the TCI (B1372/2900, Total Crystallinity Index), the HBI (B1340/B1316, Hydrogen Bond Intensity), the L/Cell index (Lignin/Cellulose, B1231/1156), the L/Hem index (Lignin/Hemicellulose, B1505/1735), the Cny/Chy index (Carbonyl (hemi)/Carbohydrate, B1735/B1368, and the Chy/Chy index (Carbohydrate/Carbohydrate, B1735/1156). These indexes are reported in existing literature (Popescu et al., 2011; Nelson et al., 1964; Poletto et al., 2012a). They were used to reveal relative shifts in biomass chemical composition and crystalline structure, by multivariate analysis (PCA, Principal Component Analysis), to discriminate the studied biomass according to the milling type procedure. The PCA analysis is a well-known algorithm to highlight the similarities and differences in a data set. To determine the set of indexes specified above, the band fitting was performed working with the OriginPro 8.5 software (OriginLab Corporation, Northampton, MA, USA) and using the Voigt function, which is the convolution of a Gaussian function and a Lorentzian function (Di Rocco, 2001; Reilly, 1992). For locating anchor points and detecting the baseline, a second derivative approach was used to do baseline corrections. To assist with parameter initialization, the baseline, peak center, and peak width parameters were fixed and released during fitting. When the best fit ($\chi^2 < 10^{-6}$) was obtained, the iteration procedure was terminated.

The thermogravimetric analyses of powdered biomass after milling, with and without LN treatment, were carried out in a C.I. Electronics Ltd. Robal electrobalance attached to a vertical furnace (1500 °C; Severn Furnaces Ltd.). 100 mg of powdered biomass samples were placed into a sintered alumina crucible. The experiments were performed using a heating rate of 10 °C min^{-1} and under argon flow (50 ml/min). Samples were heated up to 600 °C (held for 30 min) prior to natural cooling.

Cellulose (powder, CAS nº: 9004-34-6, 50 μm, Sigma-Aldrich) and lignin (CAS nº: 8068-05-1, Sigma-Aldrich), and mixtures 1:1 and 1:2, of cellulose:lignin were characterized by thermogravimetry technique and were used as reference.

The milling effect on room temperature and LN-treated biomass samples was chemically studied by an oxidative treatment. A solution of the strong oxidant sodium hypochlorite (3,5%; 50 ml) was added to 1 g of biomass powder in a round flask at 40 °C for 60 min with magnetic stirring. The residual biomass was filtered on a paper filter, extensively rinsed with distilled water, and finally dried in an oven (80 °C, overnight). The dried biomass sample was weighed to check the mass loss due to the chemical oxidation treatment.

3. Results and discussions

3.1. As-received biomass analysis

The values of the levels of nitrogen, hydrogen, carbon and sulphur (ultimate analysis) of the different biomass samples are included in Table I, as well as, the moisture content (expressed as a %wt. of the raw material). The oxygen content was estimated by the difference with the other elements. The moisture and these elements represent the biomass major component, and they fix multiple aspects of its use (Singh et al., 2017; Grandesso et al., 2011).

For each type of studied biomass, the assessment of the moisture content showed low and similar values (Cai et al., 2017). The moisture content in biomass varied in the interval of 4.9–12.6% (Table I), and in commercial compounds from 5.1% in cellulose to 10.9% in lignin, with intermediate values of 8.0% and 8.9% in the Cel:Lig 1:1 and Cel:Lig 1:2 mixtures, respectively. In overall, the moisture can fluctuate appreciably in content and, in many cases, is a troublesome ingredient (i.e. use as fuel). Several parameters in the thermal process, such as the efficiency and the temperature of combustion, the gasification process in the pyrolysis procedure at low temperature, etc. are influenced by the moisture content (Obernberger and Thek, 2004).

The farmer biomass, RicHusk, RicStr and OliPru, showed a similar moisture content (~8%). The biomass obtained from harvested wild trees, WOliPru, EucPru and PinPru, presented a higher moisture content value, approx. 11%. This may be due to the access to water for each biomass type. The farmer biomasses have access to a continued and controlled amount of water, while the wild biomass water access is in function of biomass localization (close or far from a river, dry area, etc.) and rain. Finally, the secondary products of agriculture biomass, walnut and peanut shell, showed moisture content in the range of values presented in bibliography, 8.6% and 4.9%, respectively (Lisowski et al., 2019; Perea et al., 2018).

The total ash content varies with the type of biomass source. RicHusk and RicStr samples showed an ash content (17.1% and 18.8%, respectively) greater than other samples. The other samples possess an ash content in a range of about 2.6–4.2%. The variability of ash content in the studied biomass in comparison with similar biomass found in bibliography can be explained by several factors, such as, mineral nutrients and contamination in soil or climate conditions (mean temperatures, rains, etc.) (Thomas, 1997; National Plan for Research and Technological Innovation of Spain).

If we focus our discussion on the ultimate analysis, the maximum carbon content was shown in PinePru sample, 52.47 %, and the minimum was presented by PeaShe and RicHusk samples, 40.55 and 41.24 %, respectively. The other studied samples showed a carbon content in a narrow range from 48.35% (RicStr) to 50.68% (WalShe). The highest oxygen content was shown in those samples with the lowest carbon content, RicHusk and PeaShe, 53.46 and 54.21%, respectively. The RicStr sample showed the highest hydrogen content, 10.25%, while the other sample values ranged from 5.01% to 7.21%. The nitrogen content was undetectable in the equipment used for RicHusk, PeaShe and WalShe, and it was lower than 1% for the rest of the studied samples. Regarding the sulphur content, a similar behavior was observed, undetectable for RicHusk, RicStr, WalShe, OliPru, EucPru and PinePru, and

lower than 1% for PeaShe and WOliPru samples.

The C/H ratio and high heating value (HHV) of the studied samples are also shown in Table I. The C/H ratio for each studied biomass is in the range of 4,7−8,4%. It is observed that RicHusk, PeaShe, WalShe, WOliPru, EucPru and PinePru are the richest in C/H ratio, while RicStr and Olipru showed the lowest C/H ratio values. The WalShe, WOliPru, OliPru and PinePru presented the highest HHV. No relationship was observed between both data sets. This is because the C/H ratio is determined independently of the ash or moisture content, while the HHV is calculated based on the mass of the biomass sample studied, and therefore it depends on the content of ash and moisture in the as-received biomass sample. These two characteristics vary much from one biomass sample to another, and even under the conditions in which those biomass samples have grown (soil, rains, etc.).

3.2. LN and non-LN treated milled biomass analysis

In Fig. 1 is showed the characteristic images of the studied biomasses as-received and after passing through the T_{cryo} milling treatment. The particle size distribution (PSD) results for the non-LN and the LN treated milled biomass are shown in Table II and Fig. 2. Characteristic particle volume for every biomass studied sample versus geometric average diameter in log scale, and their corresponding cumulative distribution curves are shown in Fig. 2. These characteristic cumulative undersize frequency percentages as a function of the biomass source and treatment (with and without LN) plots showed a “well graded” distribution without irregular gaps or steps for all studied samples. However, a clear trend is observed. Independently of the biomass source milled, the treatment with LN results in a significant reduction in the PSD. The LN treatment process made the fresh biomass samples less resistant to size reduction; thus, smaller particle size is obtained with lower energy consumption compared with non-LN treated milled samples.

The shape parameters, which described the asymmetry and the peakedness or flatness of the grain size distribution, were characterized by the values for graphic skewness and kurtosis. They are presented in Table II. A skewness negative value shows a tail in the negative direction (lower particle size), and in opposite, a positive value a tail in the positive direction (higher particle size). In our case, for all studied samples the values for skewness were between 0,0 and −0,3; so they can be described as symmetric or very fine skewness distribution. The negative value of the skewness corresponds to samples with a higher quantity of finer particles. The kurtosis value was between 1,0 and 1,3. A kurtosis value between 0,9 and 1,11 describes a mesokurtic distribution, and between 1,11 and 1,5 a leptokurtic distribution (Blott and Pye, 2001). The particle size distribution of the studied samples can be described as mesokurtic or slightly leptokurtic distribution. Any specific trend between skewness or kurtosis values and liquid nitrogen pretreatment was observed.

For all studied cases, LN treated biomass samples $\overline{x_D}$ were slower than those non-LN treated samples. Similar trends were observed for D_{90}, D_{50} (median diameter), and D_{10} (effective diameter) values. For all size parameter studied the size percent reduction is shown in Table II. The different percentage reduction observed in size parameters was related to the variability in chemical composition and nature of the biomass polymers. Woods and nut shell residues contain more lignin but less holocellulose (hemicellulose + cellulose) as compared to herbaceous crops or agricultural residues (Table III; values of lignin, cellulose and holocellulose content of similar biomass resources to studied samples collected from (Mohan et al., 2006; Huber et al., 2006)), and they showed a slighter particle reduction size effect due to the LN treatment. Keeping in mind the basic biomass structure, a higher content in hollocellulose (the structure pillars) led to a denser and more flexible structure (ductile), while a higher lignin content (the structure connectors) produced a more porous morphology and lower density, favoring the structure rupture by grinding media. The obtained result showed us that the cryogenization mechanism (reduction of the biomass component plasticity and, cell wall weakening by inside cells water expansion) is mainly focused on the pillars, i.e. holocellulose component, embrittlening the biomass arrangement to promote a more effective grinding procedure and to generate a lower $\overline{x_D}$. Also, the high content in ash, rich in the silicon oxide abrasive compound, helped to increase the size reduction of the coarsest rice husk and rice straw particles, when they were LN treated.

The dispersion parameter was analyzed by the geometric standard deviation (G_{SD}) and these values are shown in Table II. For all studied cases the G_{SD} was greater than 1, which is the lower limit for a wide log-normal distribution. However, a trend between LN non-LN treatment and G_{SD} was observed. Those samples treated with LN presented a lower G_{SD} value than those without LN treatment. The embrittlening of the biomass structure, produced by the cryogenization, led to a more homogenous mechanical behavior under the grinding condition, and a narrower particle size distribution for LN treated biomass sample was obtained.

In overall, LN treated biomass produced narrower and more uniform

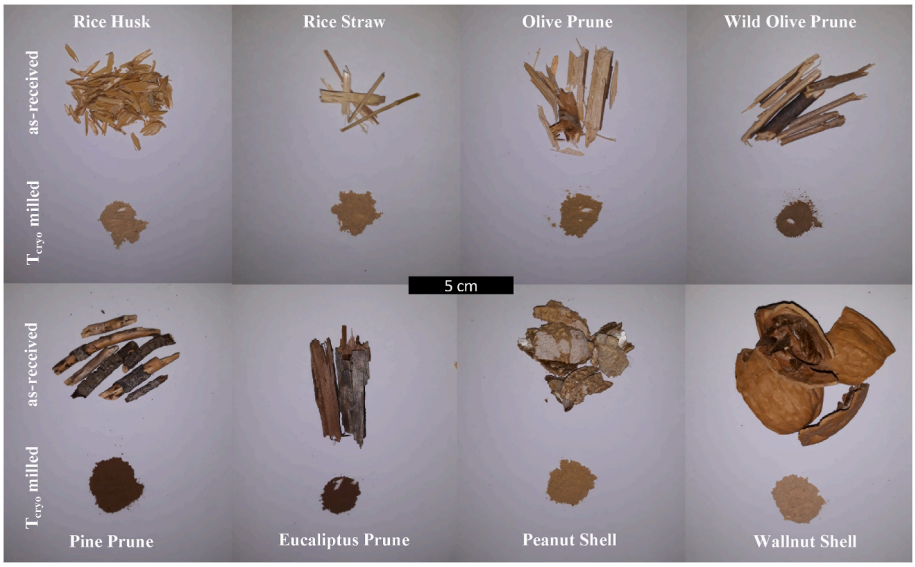

Fig. 1. The studied biomass after passing through the T_{cryo} milling pre-treatment.

Table 2
Estimated values for size, spread (sorting), symmetry (skewness) and degree of grain concentration relative to the average size (kurtosis) from grain size statistical analysis of biomass studied samples.

		RicHusk T_{room}	RicHusk T_{Cryo}	%[a]	RicStr T_{room}	RicStr T_{Cryo}	%[a]	OliPru T_{room}	OliPru T_{Cryo}	%[a]	WOliPru T_{room}	WOliPru T_{Cryo}	%[a]
Folk and Ward Method (μm)	MEAN	57,3	29,0	49,4	18,2	14,8	18,4	20,8	16,7	19,8	28,7	18,0	37,3
	G_{SD}	2,8	3,1		3,0	2,5		2,7	2,7		2,9	2.7	
	SKEWNESS	−0,3	−0,3		−0,1	−0,3		−0,3	−0,2		−0,3	−0,3	
	KURTOSIS	1,3	1,1		1,1	1,0		1,1	1,0		1,2	1,1	
Folk and Ward Method	SKEWNESS	V. Fine Lepto	V. Fine Meso		Symmetric Lepto	Fine Meso		V. Fine Lepto	Fine Meso		V. Fine Lepto	V. Fine Lepto	
	KURTOSIS												
D_{10}	(μm)	13,7	4,8	65,3	4,1	3,8	7,4	4,5	3,9	13,9	4,8	3,6	25,0
D_{50}	(μm)	65,0	35,5	45,4	19,2	17,2	10,7	25,1	19,1	23,8	37,6	22,0	41,5
D_{90}	(μm)	154,0	97,5	36,7	71,7	40,3	43,8	58,3	51,1	12,3	83,6	51,4	38,5
$(D_{90}-D_{10})/D_{50}$	(μm)	2,2	2,6		3,5	2,1		2,1	2,5				
		PinePru T_{room}	PinePru T_{Cryo}	%[a]	EucPru T_{room}	EucPru T_{Cryo}	%[a]	PeaShe T_{room}	PeaShe T_{Cryo}	%[a]	WalShe T_{room}	WalShe T_{Cryo}	%[a]
Folk and Ward Method (μm)	MEAN	28,9	26,4	8,7	34,8	23,5	32,5	19,0	13,0	31,6	35,3	29,3	17,0
	G_{SD}	2,9	2,8		2,8	2,7		3,3	3,2		4,1	2,9	
	SKEWNESS	−0,3	−0,3		−0,3	−0,3		−0,3	−0,3		0,0	−0,3	
	KURTOSIS	1,1	1,2		1,3	1,2		1,2	1,2		1,1	1,1	
Folk and Ward Method	SKEWNESS	Fine Meso	Fine Lepto		V. Fine Lepto	V. Fine Lepto		V. Fine Lepto	V. Fine Lepto		Symmetric Lepto	Fine Lepto	
	KURTOSIS												
D_{10}	(μm)	5,8	5,5	5,4	6,1	4,6	24,6	3,0	1,9	36,6	6,1	5,9	2,9
D_{50}	(μm)	33,4	30,7	7,9	43,4	28,0	35,5	23,6	16,5	30,0	36,1	33,5	7,2
D_{90}	(μm)	90,8	78,2	13,9	91,3	64,5	29,4	59,1	44,2	25,2	222,3	90,9	59,1
$(D_{90}-D_{10})/D_{50}$	(μm)	2,5	2,4								6,2	2,5	

[a] %, particle size per cent reduction from T_{Room} to T_{Cryo}.

particle size distribution compared to non-LN treated biomass samples due to the intense reduction of the biomass component plasticity and cell wall weakening caused by inside cells water expansion.

Derivate thermogravimetric (DTG) evolution profiles for studied samples are presented in Fig. 3. The chemistry of biomass is highly complex, but it can be split into its major components (lignin, cellulose, and hemicellulose) by analytical methods. Under the same pyrolysis parameters, the volatile evolution of biomass pyrolysis can be considered similar to the mixture of those of the components. The degradation temperature interval of the three main biomass components partially overlaps each other. Usually, the DTG curve can be deconvolutionated in one peak, one shoulder and one tail (Chen et al., 2015). The shoulder, at lower temperature, is related with the fastest conversion of hemicellulose and amorphous cellulose, while, the peak at higher temperature is associated with cellulose decomposition. Finally, lignin decomposed slowly over a very broad temperature range and corresponded with the curve tail (Williams and Besler, 1993; Evans and Milne, 1987a, 1987b; Kan et al., 2016; Anca-Couce et al., 2014).

Over the whole temperature range, biomass pyrolytic decomposition occurs at three stages. A first stage, from room temperature to about 140 °C, in which is observed the evaporation of moisture, the primary decomposition of more unstable compounds and the light volatiles. A second stage results in the highest mass loss and is called the biomass active pyrolysis region. This stage is caused by the biomass decomposition and it is ranged from ~140 °C to ~550 °C. Finally, a third stage (from ~550 °C to ~ 800 °C), in which, a little weight loss is observed and is related to the steady decomposition of the remaining lignin and the degradation of carbonaceous residues (Kan et al., 2016; Xun et al., 2016).

The characteristics degradation of the main components of lignocellulosic biomass takes place in stage 2, and it can be quantified through several parameters, which are related to the temperature of the peak at the maximum rate of mass loss (T_{max}) and the temperature of the main shoulder at lower temperature (T_{ms}). These temperatures for every biomass sample studied are registered in Table IV.

Regardless of the pretreatment used (non-LN or LN treatment), if the biomass samples studied are compared with previous lignocellulosic decomposition biomass literature by pyrolytic processes (Chen et al., 2015; Haiping et al., 2007; Laipeng et al., 2020; Xun et al., 2016; Garima and Thallada, 2014; Mian et al., 2016; Selim and Yıldıray, 2014; Burhennea et al., 2013), the use of a pretreatment based on high energy mechanical milling in a planetary ball mill reduced the stage 2 temperature (main phase of decomposition) about 120 °C.

When milled biomass samples, at non-LN and LN treated were compared, independently of the biomass sample source studied, as the LN-treatment was used, the DTG curve shifted, the main peak and shoulder peak, toward lower temperatures. The DTG peak temperature shifted in the range from 5 °C to 25 °C, specifically, RicHuskT_{cryo}: ~10 °C, RicStrT_{cryo}: ~10 °C, OliPruT_{cryo}: ~15 °C, WOliPruT_{cryo}: ~20 °C, PinePruT_{cryo}: ~15 °C, EucPruT_{cryo}: ~25 °C, PeaSheT_{cryo}: ~5 °C, WalSheT_{cryo}: ~25 °C. In addition to the reduction in temperature of stage 2 in LN-treated samples, another remarkable feature observed, in T_{room} vs. T_{cryo} DTG profiles, is the increment in size of the shoulder peak in comparison with de main peak. This fact implies that the lignin and cellulose degradation due to the LN-treatment led to an increment in the production of various weight lighter and more volatiles compounds, which might reach the volatilization with the hemicellulose, and the full set of volatiles decomposes intensively within the narrow temperature range. For example, this fact is clearly observed in DTG WalShe$_{Tcryo}$ biomass sample. A new peak (green circle mark) appears in DTG due to the lignin and cellulose degradation which leads to the convergence of the typical lignocellulosic biomass DTG two peaks in a lower temperature new peak.

The DTG profiles were obtained for the commercial cellulose (50 μm average size), lignin (D_{10} = 51,2, D_{50} = 100 and D_{99} = 373,3 μm particle size (D_x = %x in volume of the particles smaller than the value stated) (Abdelaziz et al., 2017) and mixtures of cellulose-lignin are presented in Fig. 4. Huge differences were found between the pyrolysis behavior of the three commercial products studied. Cellulose pyrolysis happened in a narrow temperature range from 175 °C to 235 °C, with a maximum weight loss rate at 213 °C. Over 400 °C all the cellulose was pyrolyzed. The lignin pyrolysis showed a different profile than previously analyzed samples. It decomposed over a wide temperature range from 165 °C to 590 °C. Its decomposition showed various peaks. Firstly, a double peak,

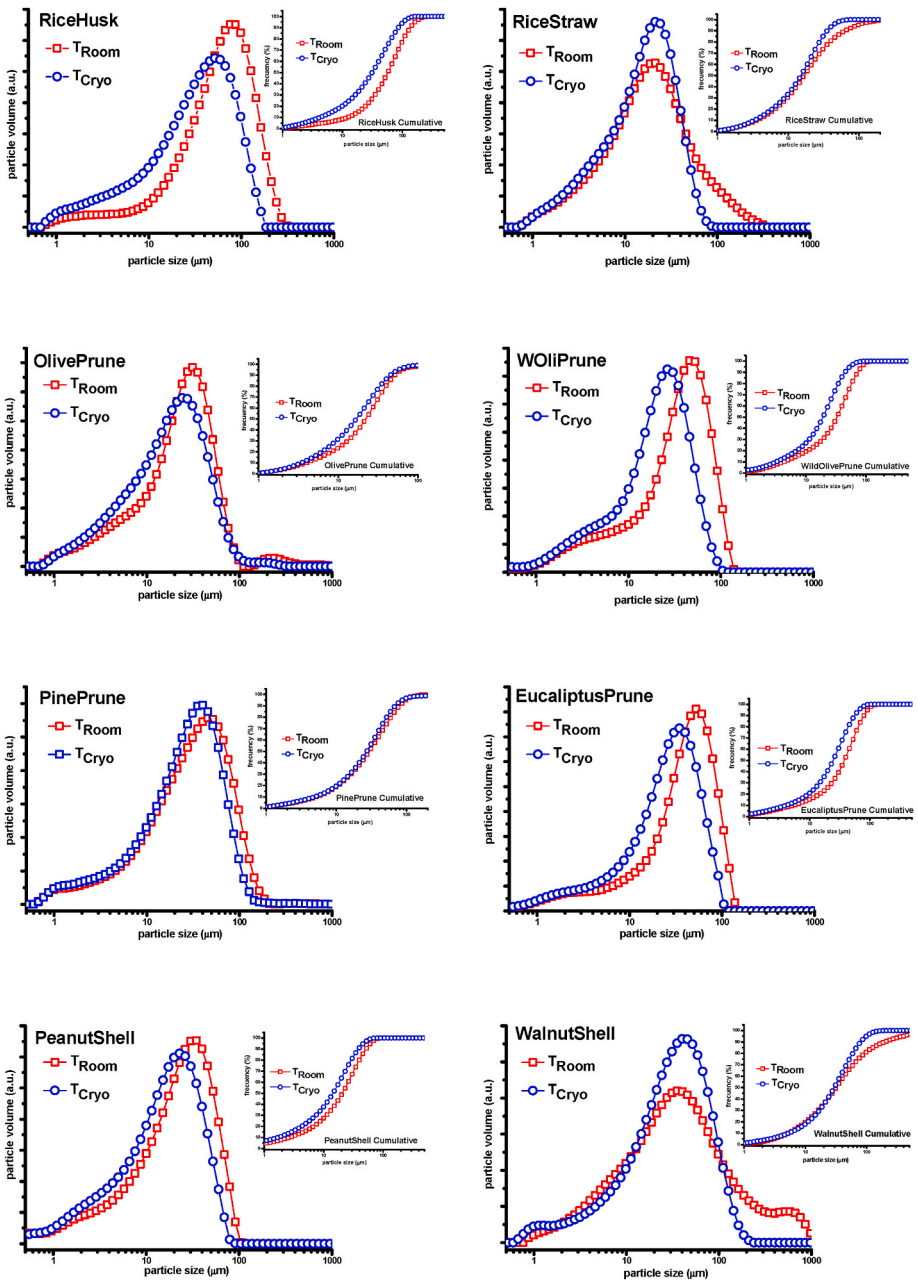

Fig. 2. Particle-size distribution cumulative undersize frequency (inset) of studied biomass.

Table 3
Chemical composition of the different lignocellulosic biomass studied in this work (Mohan et al., 2006; Huber et al., 2006).

Source	Lignin	Hemicellulose	Cellulose	Ash yield
RicHusk	18–20	24–26	34–39	~15
RicStraw	14–15	23–26	32–36	~18
OliPru	20–23	23–27	40–43	~3
WOliPru	19–22	24–26	40–44	~3
PinePru	27–29	21–23	44–46	~1.5
EucPru	25–29	18–24	42–47	~4
PeaShe	30–34	18–20	32–34	~4
WalShe	33–36	26–28	25–27	~3

with lower intensity than previous samples at 190 °C and 229 °C, secondly, a peak at 500 °C, and finally, the last one at 590 °C. The differences in the chemical nature and the structures of lignin and cellulose are mainly responsible for the different DTG behaviors found. The themogravimetric experiments with cellulose-lignin mixtures (1:1 and 1:2 ratios, respectively) showed a behavior that can be described as the weighted sum of every component partial contributions. As seen in the DTG profiles of the mixtures, the peaks were wider, shifted toward higher temperatures, and with lower intensity with the increment of lignin content in the mixture. This fact can be ascribed to the initial lignin decomposition that formed a solid shell around cellulose, which limited the heat and mass transfer during pyrolysis.

If the DTG profiles of the biomass milled samples (at T_{room} and T_{cryo}, Fig. 3) are contrasted with Fig. 4, commercial cellulose and lignin, a shifted stage 2 to lower temperatures was also observed. The reduction in temperature of stage 2 can be described in the range from 20 °C to 45 °C. This fact indicates the effectiveness of the high energy ball milling to break/degrade the highly complex main biomass components in lighter molecules. This reduction can lead to a mild conditions process (thermal or others) which drives to easier the chemical process to obtain add-value molecules.

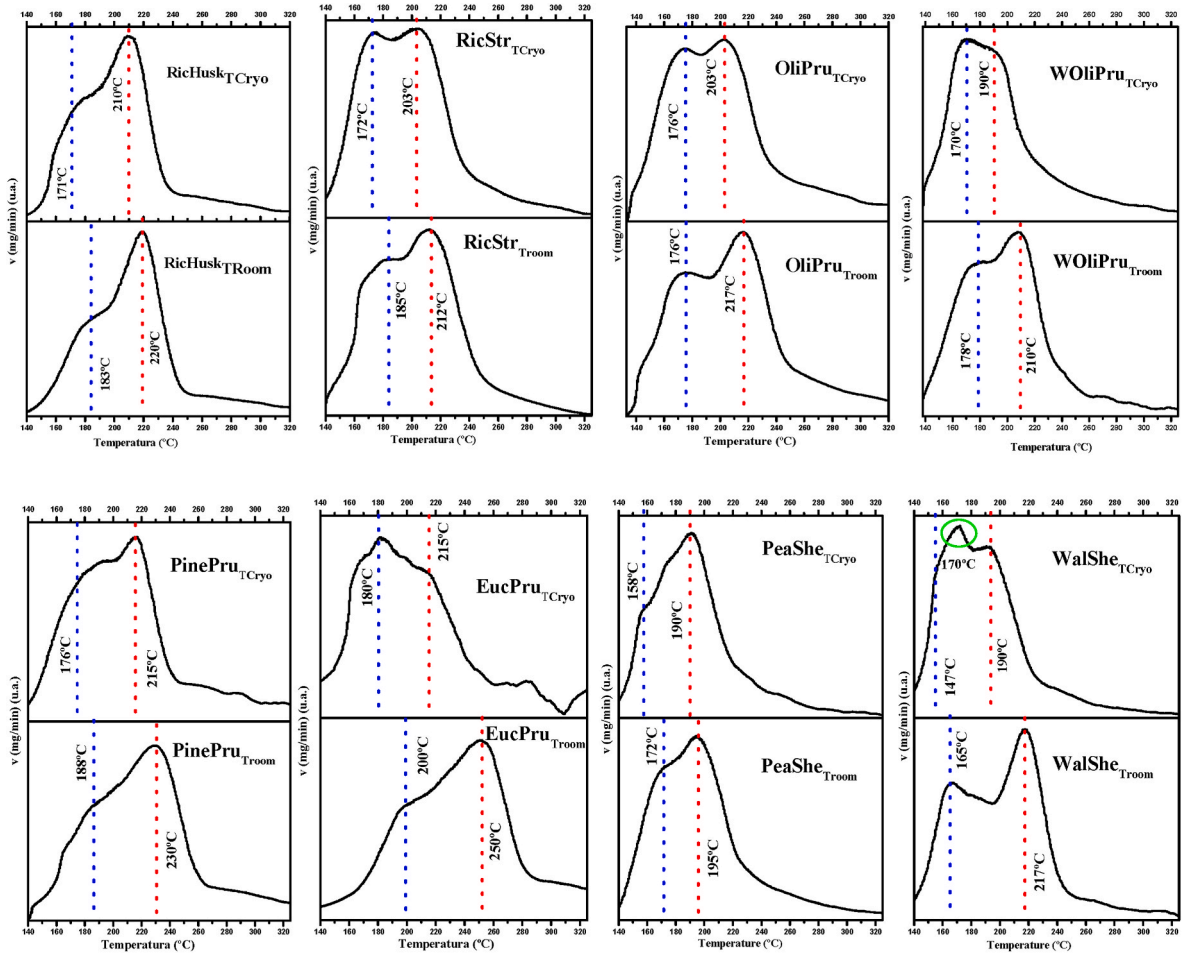

Fig. 3. DTG profiles of high energy ball milling studied samples at room temperature (T_{Room}) and under cryogenic condition (T_{Cryo}).

Table 4
Maximum temperatures (°C) of the main peak (T_{max}) and shoulder (T_{ms}) observed in pyrolyzed biomass DTG profiles. *Room* and *Cryo* temperature pretreated biomass, respectively, T_{room} and T_{cryo}. The relative standard deviation (%) for the determined temperature was 1,8.

	RicHusk	RicStr	OliPru	WOliPru	PinePru	EucPru	PeaShe	WalShe
Pretreatment	**T_{Room}**							
T_{max}	220	212	217	210	230	250	195	217
T_{ms}	183	185	176	178	188	200	172	162
Pretreatment	**T_{Cryo}**							
T_{max}	210	203	203	190	215	215	190	190
T_{ms}	171	172	176	170	176	180	155	147

The changes induced by LN-treatment in the studied biomass samples can be followed by FT-IR. This technique is a powerful tool to analyze the chemical and structural components changes generated. Any kind of these compounds, lignin, cellulose and hemicellulose, consisted mainly on aromatics, ketone C═O (1765–1715 cm^{-1}), ester (C–O–C (1270 cm^{-1})), alkene and alcohol (-OH (3400–3200 cm^{-1}, C–O–(H) (~1050 cm^{-1})) functional groups, with different oxygen content. Although they cannot be easily distinguished, still, they present different IR structures and there are signatures that can be attributed to specific components (e.g.: the band at ~1735 cm^{-1} (C═O stretching in acetyl groups and carboxylic acids) to hemicellulose; the bands at ~1595 cm^{-1}, ~1505 cm^{-1} and ~1290 cm^{-1} (C═C and C═O in-plane aromatic vibrations) to lignin; the band at ~ 1370 cm^{-1} (C–H bending) to hemicellulose and cellulose; the bands at, ~1155 cm^{-1} and ~1105 cm^{-1} (C–O–C glycosidic ether and the C–C ring breathing, respectively) to cellulose) (Schwanninger et al., 2004; Satoshi et al., 2005; Garside, 2003; Feng et al., 2013; Kondo and Dumitriu, 2005; Nishiyama et al., 2003).

The FT-IR spectra of the studied biomass samples are shown in Fig. 5. In Table V is summarized the set of empirical indexes obtained by the peak ratio analysis from the characteristics FT-IR bands. In Fig. 6 is showed the characteristic deconvoluted profiles of T_{room} and T_{cryo} RiceHusk and OliPrune samples. The LOI index is related to the total order degree in cellulose, the TCI index to the cellulose degree of crystallinity, and the HBI to the degree of intermolecular regularity. The L/Cell and L/Hemi show the ratio between lignin and carbohydrates (cellulose and hemicellulose). In a first look, LOI, TCI and HBI index showed lower values and L/Cell, L/Hemi and Cny/Chy index higher values for those samples milled under LN conditions. Finally, the Chy/Chy index remained approximately constant for both set of samples. Independently of the studied biomass these behaviors were homogeneous.

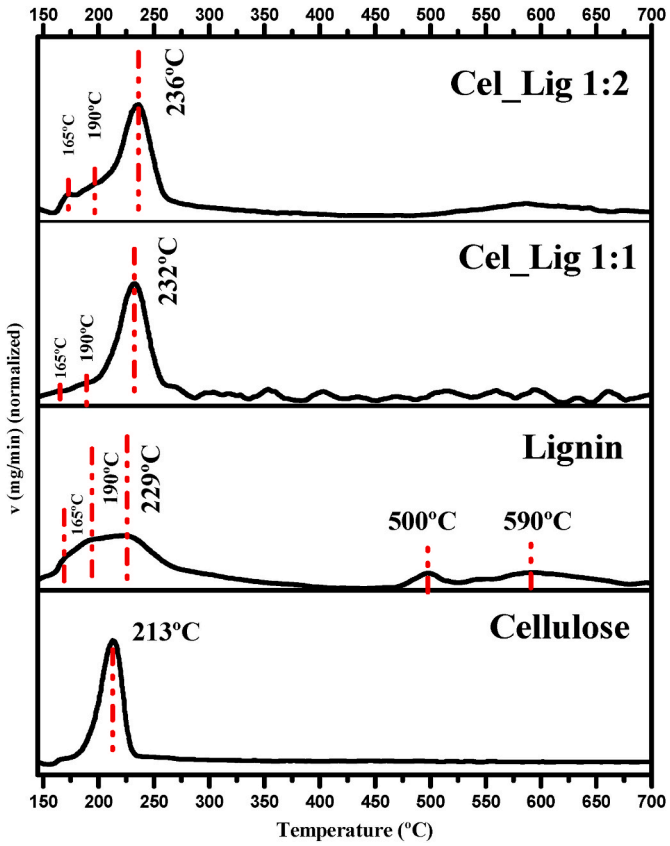

Fig. 4. DTG of Cellulose, Lignin and Cel:Lig 1:1 and Cel:Lig 1:2 mixtures.

The decreasing in LOI, TCI and HBI index values for those samples with LN-treatment showed a diminishing in the total order degree in cellulose, in the cellulose crystallinity, and in the degree of intermolecular regularity, respectively. Independently of the nature of the biomass source studied this trend is always presented and leads to the LN-treated samples to an increment in the rupture of the biomass ordered structure. A high cellulose crystallinity leads to higher thermal stability (Poletto et al., 2011, 2012b), so, the behavior observed in the thermogravimetric analysis is corroborated by the FT-IR analysis done, and in the other way around, the FT-IR analysis is corroborated by the TG behavior observed.

The slightly homogeneous increment in the L/Cell and L/Hemi index showed a higher degradation of the cellulose and hemicellulose. The two holocellulose components are more affected by the cryogenization biomass embrittlening as was analyzed above. The increment in Cny/Chy index showed an increment in carbonyl groups versus carbohydrates. And finally, the similarity between the two sets (T_{room} and T_{cryo}) of samples Chy/Chy index exhibited a homogenous behavior of cellulose and hemicellulose with the LN-treatment.

These numeric data were used to carry out the chemometric approach by PCA, and the plot result is shown in Fig. 7. The resulting scattering is shown using the scores of the first two principal components (PC) (Fig. 7(a)), preserving 36,4 and 31,1 % of the total variance, respectively. As observed in Fig. 7(a) the plot of the first two PC showed a good qualitative recognition that the non-LN treated milled biomass and LN treated milled biomass samples are well-discriminated in two groups along PC2. The LN-treated samples have mainly negative PC2 scores (represented by red circles), whereas positive PC2 scores are observed in non-LN treated milled samples (represented by blue squares). The PCA succeeded in segregating the biomass samples according to their milling pre-treatment carried out. So, this statistical methodology is helpful in confirming that the LN-treatment previous to the milling procedure induced structural and compositional changes in biomass source that led to a diminishing in cellulose crystallinity and lignin content, which reduced endemic biomass recalcitrance.

All these observed changes, induced by the pretreatment used in biomass structure and composition, can be summarized at a glance analyzing the band at 1372 cm^{-1}. This band is assigned to C–H bending deformation in cellulose and hemicellulose (Horikawa et al., 2019), and it is usually used with the 2900 cm^{-1} band for the determination of the TCI (Nelson et al., 1964). A decreasing in its intensity from non-LN treated to LN-treated biomass samples is clearly observable. The intensity band diminishing is an unambiguous signal of the reduction of the biomass crystallinity and, therefore, the biomass recalcitrance.

Finally, the oxidized residue mass, from as-received (milimetric particle size), and, LN and non-LN treated milled biomass powdered samples, obtained by hypochlorite treatment are shown in Table VI. The sodium hypochlorite produces the rupture of the biomass macromolecular structure breaking different chemical bonds and generating small molecular structures (extractable species). The lignocellulosic biomass can be converted into different smaller compounds (glucose, ketones, aromatic, etc.) after the oxidation and degradation induced by the oxidant agent. This process must be understood as the way to access to added-value products from biomass.

From data in Table VI is clearly observed the enormous weight loss presented after oxidative treatment induced by the mechanochemical pre-treatment in a planetary ball milling device. Independently of the biomass studied, the degradation of biomass large structures from as-received to milled is higher in the range from 40 to 170 % (Table VI, number in brackets), and if the room temperature milled biomass is compared to LN-treated milled biomass, this improvement in the degradation went from 2 to 20 %. Thus, the oxidation of milled biomass with sodium hypochlorite highly increased the efficiency of depolymerization, and if the biomass is previously LN-treated this improvement is even higher.

The short time high energy planetary ball milling (LN-treated better even more than non-LN treated biomass samples), has shown to play an important role in the key factors for the improvement of subsequent chemical or thermal steps. This procedure has shown a huge efficiency to induce bond cleavages, accessible surface area, structural breakage, etc. which leads to more reachable strategies for realizing the utilization of lignocellulosic biomass. A possible mechanism of the LN-treatment over the lignocellulosic biomass is showed in Fig. 8. The LN-treatment induced a glass transition on biomass polymers and favored the brittle breaking behavior. Also, the internal cell water, frozen instantaneously, can induce a high stress in lignocellulosic biomass cells by the volume expansion. Finally, this frozen water can act as blades during the first moments of the grinding.

Focusing on the LN-pre-treatment (although there is an increment in pre-treatment cost), it introduces several key factors for the potential process improvement in terms of cleaner and sustainable use of biomass as biorefineries feedstock. (1) When choosing a thermal or chemical conversion procedure, particle size, particle size distribution, particle shape, and recalcitrance reduction are important considerations. These elements, pore size, total surface area, accessibility to cellulose, and crystalline structure, are intimately related to the characteristics of biomass. Moreover, feedstock yields, properties, and processing time needs can be impacted by biomass particle sizes and recalcitrance. By influencing chemical reactivity, accessibility to biomass components, and thermal resistances (i.e., the notable variations in heat and mass transfer properties of biomass with varying particle sizes), these characteristics also influence the kinetics of the thermal process. Therefore, low recalcitrance, small size, and homogeneous distribution of particle size and shape are necessary for biomass to be used as a sustainable and reliable source of biofuel or building blocks. Although our approach still has to be adjusted, as we will mention in the section conclusion, it allows us to reduce the energy consumed during milling, which in turn lowers costs by allowing us to achieve a high-quality product in less time. (2) It is well established that the biomass moisture content leads to an

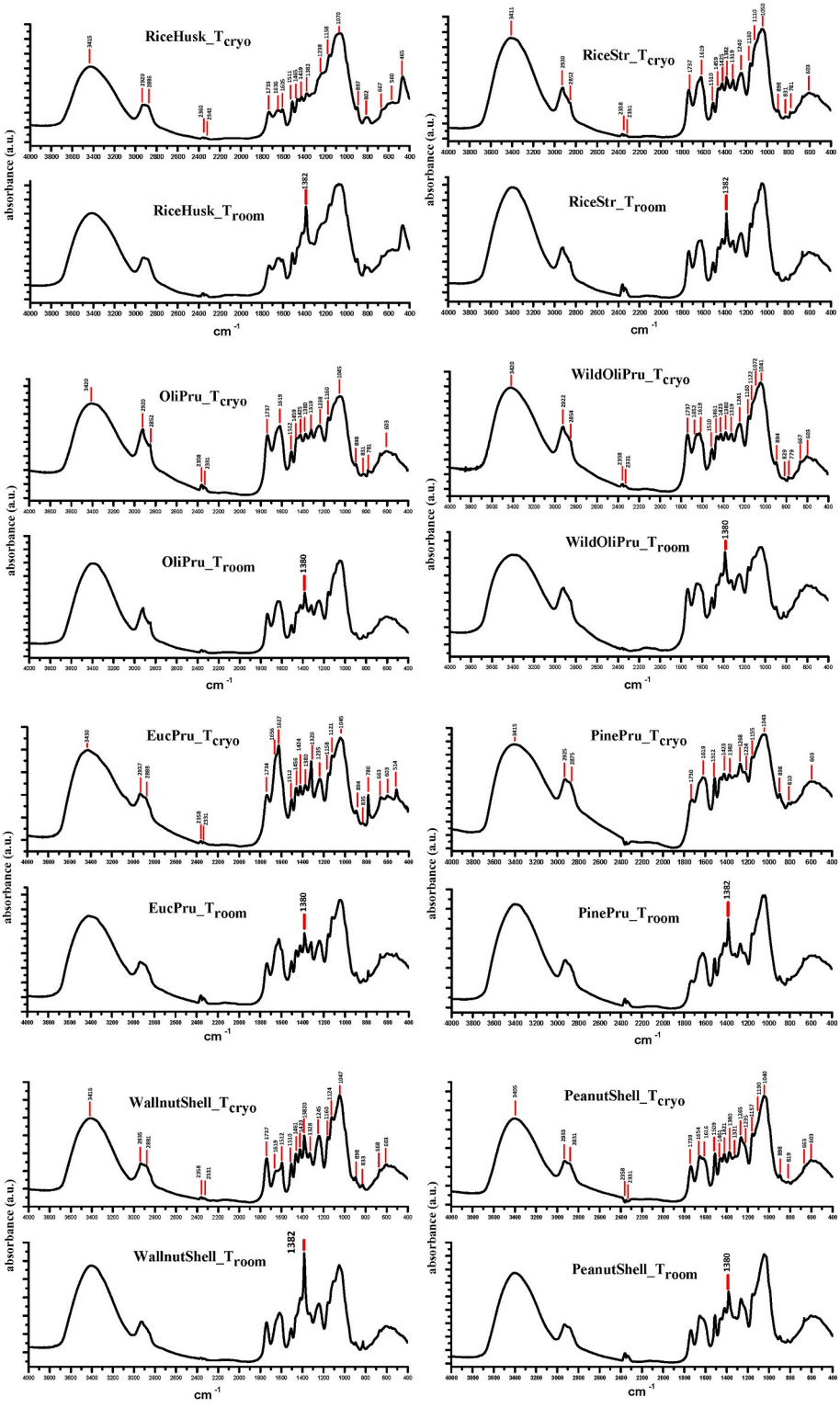

Fig. 5. FT-IR spectra of studied biomass at room temperature (T_{Room}) and under cryogenic condition (T_{Cryo}).

increment in the size reduction procedure cost. We have showed that, by a biomass LN-treatment, the moisture content can be used as an improvement in the size reduction procedure and, therefore, reducing the milling procedure cost. (3) In the way to use the biomass for an enzymatic hydrolysis treatment, LN-treatment does not introduce any kind of inhibitor. And, as we explain above, by the huge size reduction, a highly accessible cellulose product is obtained. (4) Toxic chemical waste is not produced because the lignocellulosic biomass is pre-treated without the use of harmful chemicals (cleaner production), facilitating and cheapening the next steps in the production process. (5) If thermal treatment is the next production step, as it is showed in the manuscript, TG profiles presented a significant degradation temperature reduction, reducing thermal treatment cost. (6) And finally, the TG profile of LN-treated samples presented significant changes versus non-LN treated. These changes are showing us a change in the biomass thermal degradation mechanism. This may open up fresh avenues for obtaining

Table 5
FT-IR biomass indexes from non-LN treated (T_{Room}) and LN-treated (T_{Cryo}) biomass samples. The relative standard deviation (%) for the determined index was in the range of 0,2–0,4.

FT-IR Biomass Index							
T_{Room}	LOI index. B1422/B896	TCI index. B1372/ B2900	HBI index. B3340/ B1316	L/Cell B1231/ B1156	L/Hemi B1505/ B1735	Carbonyl/Carbohy. B1735/B1372	Carbohy/Carbohy. B1735/B1156
Rice Husk	3,47	2,13	1,94	0,76	1,34	0,32	0,33
Rice Straw	5,11	1,89	2,10	0,87	0,69	0,58	0,70
Olive Prune	2,84	1,80	1,86	1,04	0,81	0,67	0,66
Wild OliPrune	4,34	1,66	2,16	0,86	0,67	0,33	0,50
Pine Prune	5,81	1,66	2,38	0,71	1,67	0,31	0,41
Eucaliptus Prune	8,04	1,92	1,46	0,76	1,36	0,41	0,87
Peanut Shell	4,29	1,30	2,37	0,81	1,32	0,60	0,53
Wallnut Shell	6,49	3,61	2,04	1,00	0,79	0,37	0,73
T_{Cryo}	LOI index. B1422/B896	TCI index. B1372/ B2900	HBI index. B3340/ B1316	L/Cell B1231/ B1156	L/Hemi B1505/ B1735	Carbonyl/Carbohy. B1735/B1372	Carbohy/Carbohy. B1735/B1156
Rice Husk	2,79	1,30	1,65	0,80	1,37	0,62	0,33
Rice Straw	3,62	1,31	1,93	0,89	0,73	0,85	0,70
Olive Prune	3,41	1,15	1,66	1,05	0,88	1,03	0,75
Wild OliPrune	2,47	0,86	2,22	0,88	0,69	0,69	0,52
Pine Prune	2,84	0,91	2,24	0,74	1,69	0,64	0,46
Eucaliptus Prune	3,68	1,25	1,25	0,78	1,39	0,78	0,74
Peanut Shell	3,13	1,11	2,06	0,85	1,34	0,76	0,57
Wallnut Shell	3,45	2,25	1,79	1,04	0,82	0,67	0,73

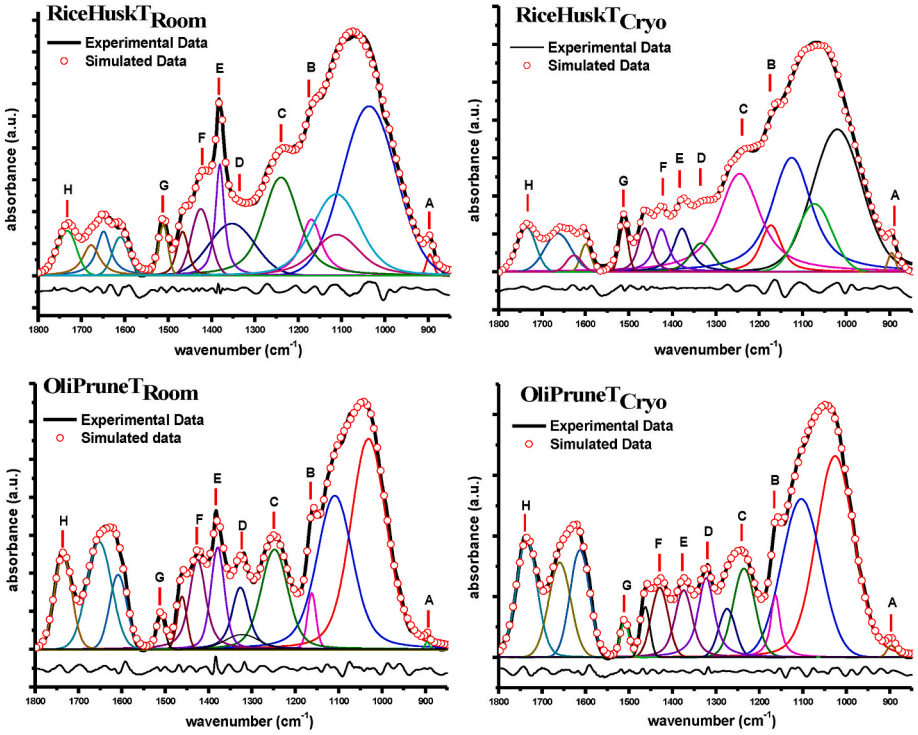

Fig. 6. Characteristics deconvoluted profiles of T_{room} and T_{cryo} RiceHusk and OliPrune. The capital letters are showing the position of the bands used to determine the calculated index. Approx. = A: 896; B:1156; C: 1231; D: 1316; E: 1368; F:1422; G: 1505; H: 1738 (cm^{-1}).

building blocks or biofuel.

4. Conclusions

A full set of different biomass sources (farmer, harvested wild tree, and secondary products) were studied. The particle size distribution, the FT-IR, the thermogravimetric, and the statistical chemometric and chemical oxidation analyses showed a remarkable reduction in biomass recalcitrance. The results have shown a high level in the rupture of the crystallinity and the depolymerization degrees of the cellulose and the lignin, for both, non-LN and LN-treated samples. The LN-treated samples even showed a higher recalcitrance reduction. The improvement in LN-treated samples can be differentiated from the non-LN treated samples by means of the analytical techniques used. It is very important to notice the changes introduced by LN-treatment in the TG profiles. This fact indicates that the LN-treatment introduces new factors that directly affect the biomass thermal degradation mechanism. This may open up fresh avenues for obtaining building blocks or biofuel.

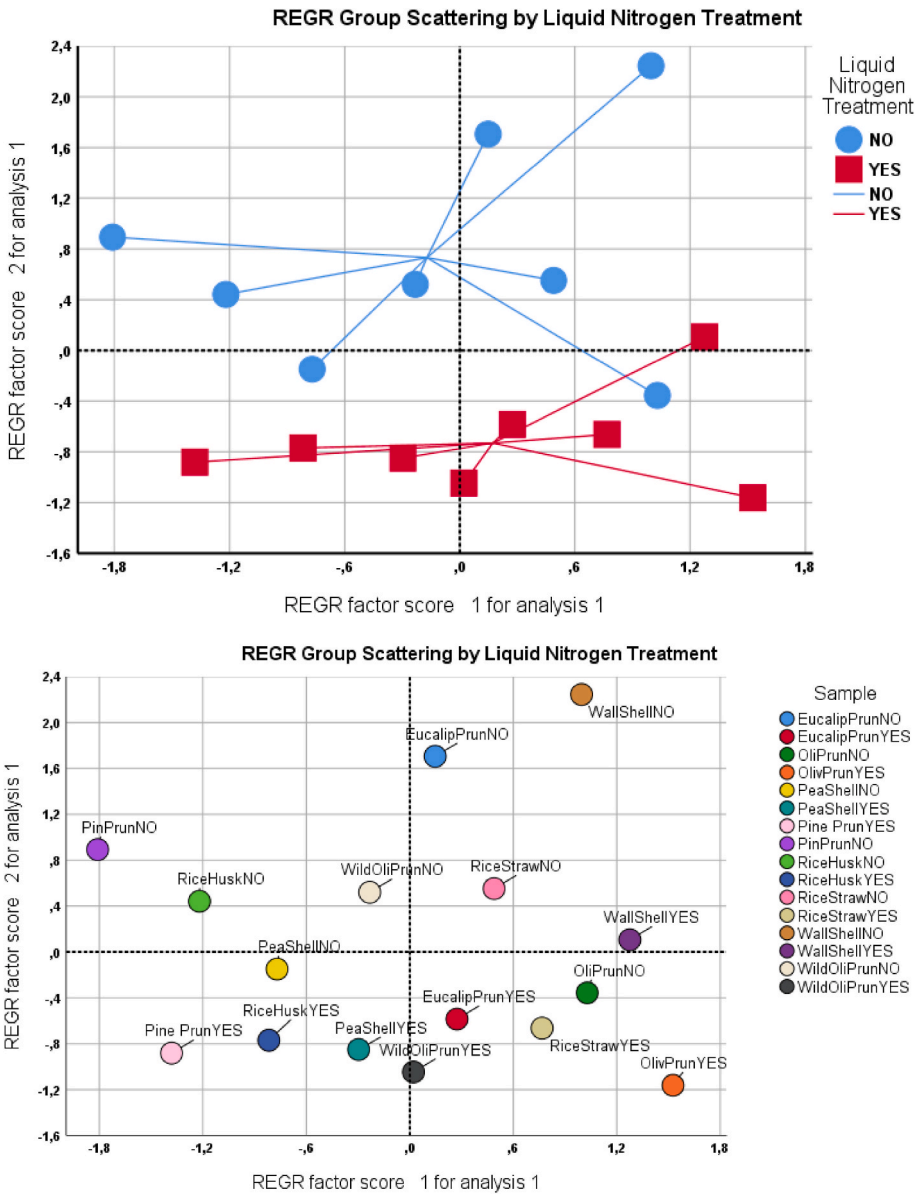

Fig. 7. PCA score plot for studied biomass samples characterized by the FT-IR biomass index.

Table 6
% wt. oxidized mass of as-received, non-LN treated (T_{Room}) and LN-treated (T_{Cryo}) biomass samples. The relative standard deviation (%) for the determined values was in the range of 1,8–2,2.

SAMPLE	% wt. oxidized mass [a]		
	as-received	Milled T_{Room}	Milled T_{Cryo}
Rice Husk	33	46 (39)	48 (45)
Rice Straw	29	52 (79)	59 (103)
Olive Prune	21	53 (152)	57 (171)
Wild OliPrune	23	54 (135)	59 (156)
Pine Prune	24	40 (66)	44 (83)
Eucaliptus Prune	24	46 (92)	51 (112)
Peanut Shell	38	64 (68)	66 (74)
Wallnut Shell	17	37 (117)	44 (159)

[a] In brackets, % improvement vs. as-received.

In summary, short time high energy planetary ball milling of non-LN and LN-treated biomass samples has proven to be a powerful tool to diminish significantly the inherent biomass recalcitrance. Also, the procedure presented can be classified in the field of green-chemistry, since any kind of environmentally unsafe chemical is required. However, to be economically viable, this LN-pretreatment must be managed in terms of energy. Because biomass feedstock has such a wide range of chemical and mechanical qualities, optimization should be done for each feedstock and mill separately. Finally, we have to note that the short-time milling used has the potential to tremendously reduce the pretreatment cost, tough further studies must be done on this point to improve the cost-effectiveness of the process by optimizing the milling time required.

CRediT authorship contribution statement

Concepción Real Pérez: Writing – review & editing, Methodology, Investigation. **María Dolores Alcalá González:** Writing – review & editing, Resources, Methodology, Investigation. **Francisca Romero Sarria:** Writing – review & editing, Methodology, Investigation. **María del Carmen Hidalgo López:** Writing – review & editing, Resources, Methodology, Investigation. **José Manuel Córdoba Gallego:** Writing – review & editing, Writing – original draft, Supervision, Software, Project administration, Methodology, Investigation, Funding acquisition,

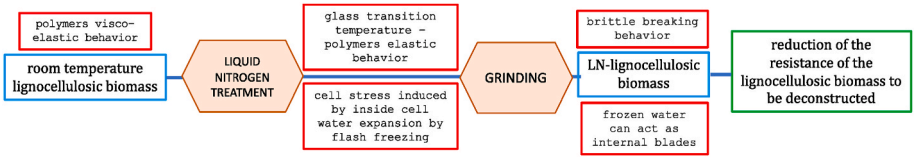

Fig. 8. Steps of a possible mechanism of the LN-treatment over the lignocellulosic biomass.

Formal analysis, Data curation, Conceptualization.

Declaration of competing interest

The authors declare that they have no known competing financial interests or personal relationships that could have appeared to influence the work reported in this paper.

Data availability

No data was used for the research described in the article.

Acknowledgments

This work wassupported by the Seville University, "Ayudas para el uso de los S.G.I., VI PPI", Project Number: 2018/00000522, and "Ayudas para el uso de los S.G.I., VII P.P.I.", Project Number: 2022/00000259. Proyectos Generación del Conocimiento PID 2021-122413NB-I00, Ministerio de Ciencia e Innovación.

The authors want to thank the invaluable help of the laboratory technician Rosa María Ojeda Carrillo for her help in the goals achieving.

References

Abdelaziz, O.Y., Hulteberg, C.P., 2017. Physicochemical characterisation of technical lignins for their potential valorisation. Waste Biomass Valor 8, 859–869. https://doi.org/10.1007/s12649-016-9643-9.

An, Y.X., Zong, M.H., et al., 2015. Pretreatment of lignocellulosic biomass with renewable cholinium ionic liquids: biomass fractionation, enzymatic digestion and ionic liquid reuse. Bioresour. Technol. 192, 165–171. https://doi.org/10.1016/j.biortech.2015.05.064.

Anca-Couce, A., Berger, A., et al., 2014. How to determine consistent biomass pyrolysis kinetics in a parallel reaction scheme. Fuel 123, 230–240. https://doi.org/10.1016/j.fuel.2014.01.014.

Arce, C., Kratky, L., 2022. Mechanical pretreatment of lignocellulosic biomass toward enzymatic/fermentative valorization. iScience 25 (7), 104610. https://doi.org/10.1016/j.isci.2022.104610.

Bals, B., Rogers, C., et al., 2010. Evaluation of ammonia fibre expansion (AFEX) pretreatment for enzymatic hydrolysis of switchgrass harvested in different seasons and locations. Biotechnol. Biofuels 3, 1. https://doi.org/10.1186/1754-6834-3-1.

Barakat, A., de Vries, H., et al., 2013. Dry fractionation process as an important step in current and future lignocellulose biorefineries: a review. Bioresour. Technol. 134, 362–373. https://doi.org/10.1016/j.biortech.2013.01.169.

Blott, S.J., Pye, K., 2001. GRADISTAT: a grain size distribution and statistics package for the analysis of unconsolidated sediments. Earth Surf. Process. Landforms 26, 1237–1248. https://doi.org/10.1002/esp.261.

Brodeur, G., Yau, E., et al., 2011. Chemical and physiocochemical pretreatment of lignocellulosic biomass. A review. Enzym. Res. 1–17 https://doi.org/10.4061/2011/787532.

Broer, K.M., Peterson, C., 2019. Gasification. In: Brown, R. (Ed.), Thermochemical Processing of Biomass. https://doi.org/10.1002/9781119417637.

Burhennea, L., Messmer, J., et al., 2013. The effect of the biomass components lignin, cellulose and hemicellulose on TGA and fixed bed pyrolysis. J. Anal. Appl. Pyrol. 101, 177–184. https://doi.org/10.1016/j.jaap.2013.01.012.

Cai, J., et al., 2017. Review of physicochemical properties and analytical characterization of lignocellulosic biomass. Renew. Sustain. Energy Rev. 76, 309–322. https://doi.org/10.1016/j.rser.2017.03.072.

Chen, Z., et al., 2015. Characteristics and kinetic study on pyrolysis of five lignocellulosic biomass via thermogravimetric analysis. Bioresour. Technol. 192, 441–450. https://doi.org/10.1016/j.biortech.2015.05.062.

Di Rocco, H.O., 2001. General expression for the Voigt function that is of special interest for applied spectroscopy. Appl. Spectrosc. 55, 822–826. https://opg.optica.org/as/abstract.cfm?URI=as-55-7-822.

Dubey, A.K., Gupta, P.K., et al., 2012. Bioethanol production from waste paper acid pretreated hydrolyzate with xylose fermenting Pichia stipitis. Carbohydr. Polym. 88, 825–829. https://doi.org/10.1016/j.carbpol.2012.01.004.

Evans, R.J., Milne, T.A., 1987a. Molecular characterization of the pyrolysis of biomass. 1. Fundamentals. Energy Fuels 1 (2), 123–137. https://doi.org/10.1021/ef00002a001.

Evans, R.J., Milne, T.A., 1987b. Molecular characterization of the pyrolysis of biomass. 2. Applications. Energy Fuels 1 (2), 311–319. https://doi.org/10.1021/ef00004a001.

Fan, L.T., Lee, Y.-H., et al., 2010. The nature of lignocellulosics and their pretreatments for enzymatic hydrolysis. Adv. Biochem. Eng. 23, 157–187. https://doi.org/10.1007/3540116982_4.

Feng, X., Jianming, Y., et al., 2013. Qualitative and quantitative analysis of lignocellulosic biomass using infrared techniques: a mini-review. Appl. Energy 104, 801–809. https://doi.org/10.1016/j.apenergy.2012.12.019.

Garima, M., Thallada, B., 2014. Non-isothermal model free kinetics for pyrolysis of rice straw. Bioresour. Technol. 169, 614–621. https://doi.org/10.1016/j.biortech.2014.07.045.

Garside, P., 2003. Identification of cellulosic fibres by FTIR spectroscopy. Studies in conservation. Taylor & Francis, Ltd. 48 (4), 269–275. https://doi.org/10.1179/sic.2003.48.4.269.

Goswami, T.K., Singh, M., 2003. Role of feed rate and temperature in attrition grinding of cumin. J. Food Eng. 59, 285–290. https://doi.org/10.1016/S0260-8774(02)00469-7.

Gould, J.M., 1984. Alkaline peroxide delignification of agricultural residues to enhance enzymatic saccharification. Biotechnol. Bioeng. 26, 46–52. https://doi.org/10.1002/bit.260260110.

Grandesso, E., et al., 2011. Effect of moisture, charge size, and chlorine concentration on PCDD/F emissions from simulated open burning of forest biomass. Environ. Sci. Technol. 45, 3887–3894. https://doi.org/10.1021/es103686t.

Haiping, Y., et al., 2007. Characteristics of hemicellulose, cellulose and lignin pyrolysis. Fuel 86, 1781–1788. https://doi.org/10.1016/j.fuel.2006.12.013.

Hemery, Y., et al., 2011. Potential of dry fractionation of wheat bran for the development of food ingredients, part I: influence of ultra-fine grinding. J. Cereal. Sci. 53, 1–8. https://doi.org/10.1016/j.jcs.2010.09.005.

Horikawa, Y., et al., 2019. Prediction of lignin contents from infrared spectroscopy: chemical digestion and lignin/biomass ratios of cryptomeria japonica. Appl. Biochem. Biotechnol. 188, 1066–1076. https://doi.org/10.1007/s12010-019-02965-8.

Huber, G.W., et al., 2006. Synthesis of transportation fuels from biomass: chemistry, catalysts, and engineer. Chem. Rev. 106, 4044–4098. https://doi.org/10.1021/cr068360d.

Kan, T., Strezov, V., Evans, T.J., 2016. Lignocellulosic biomass pyrolysis. A review of product properties and effects of pyrolysis parameters. Renew. Sustain. Energy Rev. 57, 1126–1140. https://doi.org/10.1016/j.rser.2015.12.185.

Kondo, T., 2005. Hydrogen bonds in cellulose and cellulose derivatives. In: Dumitriu, S. (Ed.), Polysaccharides II – Structural Diversity and Functional Versatility. Marcel Dekker, New York, pp. 69–99. https://doi.org/10.1201/9781420030822-7. ISBN: 9780429131660.

Kristiani, A., et al., 2015. Effect of combining chemical and irradiation pretreatment process to characteristic of oil palm's empty fruit bunches as raw material for second generation bioethanol. Energy Proc. 68, 195–204. https://doi.org/10.1016/j.egypro.2015.03.248.

Laipeng, L., et al., 2020. Insight into pyrolysis kinetics of lignocellulosic biomass: isoconversional kinetic analysis by the modified Friedman method. Energy Fuels 34, 4874–4881. https://doi.org/10.1021/acs.energyfuels.0c00275.

Lisowski, A., et al., 2019. Effects of moisture content, temperature, and die thickness on the compaction process, and the density and strength of walnut shell pellets. Renew. Energy 141, 770–781. https://doi.org/10.1016/j.renene.2019.04.050.

Manohar, B., Sridhar, B.S., 2003. Size and shape characterization of conventionally and cryogenically ground turmeric (Curcuma domestica) particles. Powder Technol. 120, 292–297. https://doi.org/10.1016/S0032-5910(01)00284-4.

McGinnis, G.D., Wilson, W.W., et al., 1983. Biomass pretreatment with water and high-pressure oxygen. The wet-oxidation process. Ind. Eng. Chem. Prod. Res. Dev. 22, 352–357. https://doi.org/10.1021/i300010a036.

Mian, H., et al., 2016. Thermogravimetric kinetics of lignocellulosic biomass slow pyrolysis using distributed activation energy model, Fraser–Suzuki deconvolution, and iso-conversional method. Energy Convers. Manag. 118, 1–11. https://doi.org/10.1016/j.enconman.2016.03.058.

Mohan, D., et al., 2006. Pyrolysis of wood/biomass for bio-oil: a critical review. Energy Fuels 20 (3), 848–889. https://doi.org/10.1021/ef0502397.

Mulakhudair, A.R., Hanotu, J., et al., 2017. Exploiting ozonolysis-microbe synergy for biomass processing: application in lignocellulosic biomass pretreatment. Biomass Bioenergy 2017, 147–154. https://doi.org/10.1016/j.biombioe.2017.06.018.

Mussatto, S.I., Teixeira, J.A., 2010. Lignocellulose as raw material in fermentation processes. Curr Res Technol Educ Top Appl Microbiol Microb Biotechnol Méndez-Vilas Ed. 2, 897–907. ISBN: 8461461959.

Nair, L.G., Agrawal, K., et al., 2023. Organosolv pretreatment: an in-depth purview of mechanics of the system. Bioresour. Bioprocess. 10, 50. https://doi.org/10.1186/s40643-023-00673-0.

National Plan for Research and Technological Innovation of Spain (2021-27).https://www.ciencia.gob.es/Estrategias-y-Planes/Planes-y-programas/PEICTI.html.
Nelson, M.L., O'Connor, R.T., 1964. Relation of certain infrared bands to cellulose crystallinity and crystal lattice type. Part II. A new infrared ratio for estimation of crystallinity in celluloses I and II. J. Appl. Polym. Sci. 8, 1325–1341. https://doi.org/10.1002/app.1964.070080323.
Nishiyama, Y., Sugiyama, J., et al., 2003. Crystal structure and hydrogen bonding system in cellulose iα from synchrotron X-ray and neutron fiber diffraction. J. Am. Chem. Soc. 125, 14300–14306. https://doi.org/10.1021/ja0257319.
Obernberger, I., Thek, G., 2004. Physical characterization and chemical composition of densified biomass fuels with regard to their combustion behaviour. Biomass Bioenergy 27, 653–669. https://doi.org/10.1016/j.biombioe.2003.07.006.
Perea-Moreno, M.A., et al., 2018. Peanut shell for energy: properties and its potential to respect the environment. Sustainability 10, 3254–3269. https://doi.org/10.3390/su10093254.
Poletto, M., Pistor, V., et al., 2011. Crystalline properties and decomposition kinetics of cellulose fibers in wood pulp obtained by two pulping processes. Polym. Degrad. Stabil. 96 (4), 679–685. https://doi.org/10.1016/j.polymdegradstab.2010.12.007.
Poletto, M., Zattera, A.J., et al., 2012a. Structural differences between wood species: evidence from chemical composition, FTIR spectroscopy, and thermogravimetric analysis. J. Appl. Polym. Sci. 126, E337–E344. https://doi.org/10.1002/app.36991.
Poletto, M., Zattera, A.J., et al., 2012b. Thermal decomposition of wood: influence of wood components and cellulose crystallite size. Bioresour. Technol. 109, 148–153. https://doi.org/10.1016/j.biortech.2011.11.122.
Popescu, M.C., Popescu, C.M., et al., 2011. Evaluation of morphological and chemical aspects of different wood species by spectroscopy and thermal methods. J. Mol. Struct. 988 (1–3), 65–72. https://doi.org/10.1016/j.molstruc.2010.12.004.
Reilly, J.T., 1992. Analysis of FT-IR spectroscopic data: the Voigt profile. Spectrochim. Acta 48A (10), 1459–1479. https://doi.org/10.1016/0584-8539(92)80154-O.
Saini, J.K., Saini, R., Tewari, L., 2015. Lignocellulosic agriculture wastes as biomass feedstocks for second-generation bioethanol production: concepts and recent developments. Biotechnology 5, 337–353. https://doi.org/10.1007/s13205-014-0246-5.
Satoshi, K., Kadla, J.F., 2005. Hydrogen bonding in lignin. A Fourier transform infrared model compound study. Biomacromolecules 6, 2815–2821. https://doi.org/10.1021/bm050288q.
Sawant, S.S., Salunke, B.K., et al., 2016. Lignocellulosic and marine biomass as resource for production of polyhydroxyalkanoates. Kor. J. Chem. Eng. 33, 1505–1513. https://doi.org/10.1007/s11814-016-0019-4.
Saxena, V., et al., 2018. Improving quality of cumin powder through cryogenic grinding technology. J. Food Process. Preserv. 42, 13371 https://doi.org/10.1111/jfpp.13371.
Schwanninger, M., Rodrigues, J.C., et al., 2004. Effects of short-time vibratory ball milling on the shape of FT-IR spectra of wood and cellulose. Vib. Spectrosc. 36, 23–40. https://doi.org/10.1016/j.vibspec.2004.02.003.
Selim, C., Yıldıray, T., 2014. Pyrolysis kinetics of hazelnut husk using thermogravimetric analysis. Bioresour. Technol. 156, 182–188. https://doi.org/10.1016/j.biortech.2014.01.040.
Singh, K.K., Goswami, T.K., 1999. Studies on cryogenic grinding of cumin seed. J. Food Process. Eng. 22, 175–190. https://doi.org/10.1111/j.1745-4530.1999.tb00479.x.
Singh, Y.D., Mahanta, P., et al., 2017. Comprehensive characterization of lignocellulosic biomass through proximate, ultimate and compositional analysis for bioenergy production. Renew. Energy 103, 490–500. https://doi.org/10.1016/j.renene.2016.11.039.
Stewart, M.L., Slavin, J.L., 2009. Particle size and fraction of wheat bran influence short-chain fatty acid production in vitro. Br. J. Nutr. 102 (10), 1404–1407. https://doi.org/10.1017/S0007114509990663.
Subhedar, P.B., Gogate, P.R., 2016. Chapter 6 - use of ultrasound for pretreatment of biomass and subsequent hydrolysis and fermentation. In: Mussatto, Solange I. (Ed.), Biomass Fractionation Technologies for a Lignocellulosic Feedstock Based Biorefinery. Elsevier, pp. 127–149. https://doi.org/10.1016/B978-0-12-802323-5.00006-2. ISBN 9780128023235.
Taherzadeh, M.J., Karimi, K., 2008. Pretreatment of lignocellulosic wastes to improve ethanol and biogas production: a review. Int. J. Mol. Sci. 9 (9), 1621–1651. https://doi.org/10.3390/ijms9091621.
Thomas, K.M., 1997. The release of nitrogen oxides during char combustion. Fuel 76, 457–473. https://doi.org/10.1016/S0016-2361(97)00008-2.
Vargas-Moreno, J.M., et al., 2012. A review of the mathematical models for predicting the heating value of biomass materials. Renew. Sustain. Energy Rev. 16, 3065–3083. https://doi.org/10.1016/j.rser.2012.02.054.
Williams, P.T., Besler, S., 1993. The pyrolysis of rice husks in a thermogravimetric analyzer and static batch reactor. Fuel 72, 151–159. https://doi.org/10.1016/0016-2361(93)90391-E.
Xun, W., et al., 2016. Thermogravimetric kinetic study of agricultural residue biomass pyrolysis based on combined kinetics. Bioresour. Technol. 219, 510–520. https://doi.org/10.1016/j.biortech.2016.07.136.
Zhang, L., Xu, C.C., et al., 2010. Energy recovery from secondary pulp/paper-mill sludge and sewage sludge with supercritical water treatment. Bioresour. Technol. 101, 2713–2721. https://doi.org/10.1016/j.biortech.2009.11.106.
Ziegler-Devin, I., Chrusciel, L., Brosse, N., 2021. Steam explosion pretreatment of lignocellulosic biomass: a mini-review of theatrical and experimental approaches. Front. Chem. 9, 705358 https://doi.org/10.3389/fchem.2021.705358.
Zoghlami, A., Paës, G., 2019. Lignocellulosic biomass: understanding recalcitrance and predicting hydrolysis. Front. Chem. 7, 874. https://doi.org/10.3389/fchem.2019.00874.